# Diabetic Nephropathy Is Accelerated by Farnesoid X Receptor Deficiency and Inhibited by Farnesoid X Receptor Activation in a Type 1 Diabetes Model

**Xiaoxin X. Wang,[1] Tao Jiang,[1] Yan Shen,[1] Yupanqui Caldas,[1] Shinobu Miyazaki-Anzai,[1] Hannah Santamaria,[1] Cydney Urbanek,[1] Nathaniel Solis,[1] Pnina Scherzer,[2] Linda Lewis,[1] Frank J. Gonzalez,[3] Luciano Adorini,[4] Mark Pruzanski,[5] Jeffrey B. Kopp,[6] Jill W. Verlander,[7] and Moshe Levi[1]**

**OBJECTIVE—**The pathogenesis of diabetic nephropathy is complex and involves activation of multiple pathways leading to kidney damage. An important role for altered lipid metabolism via sterol regulatory element binding proteins (SREBPs) has been recently recognized in diabetic kidney disease. Our previous studies have shown that the farnesoid X receptor (FXR), a bile acid-activated nuclear hormone receptor, modulates renal SREBP-1 expression. The purpose of the present study was then to determine if FXR deficiency accelerates type 1 diabetic nephropathy in part by further stimulation of SREBPs and related pathways, and conversely, if a selective FXR agonist can prevent the development of type 1 diabetic nephropathy.

**RESEARCH DESIGN AND METHODS—**Insulin deficiency and hyperglycemia were induced with streptozotocin (STZ) in C57BL/6 FXR KO mice. Progress of renal injury was compared with nephropathy-resistant wild-type C57BL/6 mice given STZ. DBA/2J mice with STZ-induced hyperglycemia were treated with the selective FXR agonist INT-747 for 12 weeks. To accelerate disease progression, all mice were placed on the Western diet after hyperglycemia development.

**RESULTS—**The present study demonstrates accelerated renal injury in diabetic FXR KO mice. In contrast, treatment with the FXR agonist INT-747 improves renal injury by decreasing proteinuria, glomerulosclerosis, and tubulointerstitial fibrosis, and modulating renal lipid metabolism, macrophage infiltration, and renal expression of SREBPs, profibrotic growth factors, and oxidative stress enzymes in the diabetic DBA/2J strain.

**CONCLUSIONS—**Our findings indicate a critical role for FXR in the development of diabetic nephropathy and show that FXR activation prevents nephropathy in type 1 diabetes. ***Diabetes*** **59:2916–2927, 2010**

From the [1]Department of Medicine, University of Colorado Denver, and the VA Medical Center, Aurora, Colorado; the [2]Nephrology and Hypertension Services, Hadassah University Hospital, Jerusalem, Israel; the [3]Laboratory of Metabolism, Center for Cancer Research, National Cancer Institute, National Institutes of Health, Bethesda, Maryland; [4]Intercept Pharmaceuticals, Perugia, Italy; [5]Intercept Pharmaceuticals, New York, New York; the [6]Kidney Disease Section, National Institute of Diabetes and Digestive and Kidney Diseases, National Institutes of Health, Bethesda, Maryland; and the [7]Department of Medicine, Division of Nephrology, Hypertension, and Transplantation, University of Florida, Gainesville, Florida.

Corresponding author: Moshe Levi, moshe.levi@ucdenver.edu.

Received 6 January 2010 and accepted 28 July 2010. Published ahead of print at http://diabetes.diabetesjournals.org on 10 August 2010. DOI: 10.2337/db10-0019.

X.X.W. and T.J. contributed equally to this work.



Diabetic nephropathy is the most common renal complication of diabetes and the leading cause of end-stage renal disease (1). The pathogenesis of diabetic nephropathy is complex and involves activation of multiple pathways leading to kidney damage, including the polyol pathway, advanced glycation end products, oxidative stress, proinflammatory cytokines, and profibrotic growth factors (2,3). In addition, an important role for altered lipid metabolism has been recently recognized in diabetic kidney disease (4–8). In this condition, there is increased renal expression of sterol regulatory element binding proteins 1 and 2 (SREBP-1 and SREBP-2), transcription factors that mediate increased fatty acid and cholesterol synthesis, resulting in triglyceride and cholesterol accumulation in the kidney and are associated with inflammation, oxidative stress, fibrosis, and proteinuria. We have established a critical role for SREBP-1 by determining that SREBP-1 transgenic mice develop glomerulosclerosis and proteinuria in the absence of alterations in serum glucose or lipids, and that SREBP-1c knockout mice are protected from the renal effects of a high-fat diet (4,9).

Modulation of SREBPs may therefore represent a rational approach to prevent diabetic renal complications. Since SREBP-1 or SREBP-2 inhibitors are still unavailable, we have focused on the potential role of the farnesoid X receptor (FXR), a bile acid-activated nuclear hormone receptor which modulates SREBP-1 expression (10,11). Indeed, our previous studies have shown that FXR agonists decrease SREBP-1c expression in the kidney (7,12).

The purpose of the present study was then to determine if FXR deficiency accelerates type 1 diabetic nephropathy in part by further stimulation of SREBP and related pathways, and conversely, if a selective FXR agonist can prevent the development of type 1 diabetic nephropathy.

## RESEARCH DESIGN AND METHODS

Homozygous male FXR knockout mice (FXR KO) of 6 months of age backcrossed onto the C57BL/6 genetic background for 10 generations (13), sex- and age-matched C57BL/6 wild-type mice, and 8-week-old male DBA2/J mice were all obtained from Jackson Laboratories (Bar Harbor, ME). They were maintained on a 12-h light/12-h dark cycle. The deletion of FXR was confirmed with genotyping and Western blot (supplemental Fig. S1, available in the online appendix at http://diabetes.diabetesjournals.org/cgi/content/full/db10-0019/DC1). Mice were injected with streptozotocin (STZ) (Sigma-Aldrich, St. Louis, MO) intraperitoneally (40 mg/kg for DBA/2J and 50 mg/kg for C57BL/6 strains, freshly made in 50 mmol/l sodium citrate buffer, pH 4.5) for 5 consecutive days, or with 50 mmol/l sodium citrate solution only. Tail vein blood glucose levels were measured 1 week after the last STZ injection, and

TABLE 1
Metabolic data in normoglycemic control and diabetic FXR KO mice

| | WT | FXR KO | WT + STZ | FXR KO + STZ |
|---|---|---|---|---|
| Body weight (g) | 44.2 ± 2.28 | 41.0 ± 1.98 | 28.4 ± 0.95[a] | 25.0 ± 1.27 |
| Kidney weight (g) | 0.36 ± 0.02 | 0.34 ± 0.01 | 0.38 ± 0.01 | 0.37 ± 0.01 |
| Kidney/body weight ratio (%) | 0.82 ± 0.02 | 0.84 ± 0.02 | 1.33 ± 0.06[a] | 1.48 ± 0.09 |
| Plasma glucose (mg/dl) | 193 ± 15 | 183 ± 12 | 769 ± 81 | 731 ± 85 |
| Plasma TG (mg/dl) | 12.7 ± 3.42 | 32.9 ± 6.20[a] | 54.4 ± 8.73[a] | 1,081 ± 603[bc] |
| Plasma TC (mg/dl) | 308 ± 25 | 487 ± 28[a] | 334 ± 38 | 1,217 ± 99[bc] |
| Plasma HDL-C (mg/dl) | 123 ± 9 | 181 ± 15[a] | 83.8 ± 2.4[a] | 26.3 ± 2.6[bc] |
| Plasma LDL-C (mg/dl) | 124 ± 14 | 202 ± 18[a] | 132 ± 17 | 905 ± 86[bc] |
| Plasma insulin (ng/ml) | 2.75 ± 0.37 | 2.25 ± 0.06 | 0.49 ± 0.06[a] | 0.64 ± 0.12[c] |
| Urine ACR (mg/g) | 25.4 ± 3.8 | 59.4 ± 11.2[a] | 30.7 ± 5.4 | 328 ± 66[bc] |
| Glomerular volume ($\mu m^2$) | 3,286 ± 168 | 4,243 ± 179[a] | 4,129 ± 154[a] | 5,457 ± 263[bc] |

Data are means ± SE ($n = 6$ mice in each group): [a]$P < 0.05$ vs. WT + WD, [b]$P < 0.05$ vs. WT + STZ/WD, [c]$P < 0.05$ vs. FXR KO/WD. ACR, albumin/creatinine ratio; HDL-C, HDL cholesterol; LDL-C, LDL cholesterol; TC, total cholesterol; TG, triglyceride; WT, wild-type.

mice with glucose levels >250 mg/dl were considered diabetic. FXR KO mice and their wild-type counterparts were fed with a high-fat high-cholesterol Western diet (WD, TD88137) obtained from Harlan-Teklad (Madison, WI) after the onset of diabetes and were studied after 12 weeks of diabetes. DBA/2J mice were fed WD after the onset of diabetes in STZ groups and were treated for 8 weeks with: *1*) WD only; *2*) the semisynthetic FXR agonist 6-α-ethyl-chenodeoxycholic acid (INT-747, Intercept Pharmaceuticals, New York, NY) (14): 30 mg/kg body weight admixed with WD. Animal studies and relative protocols were approved by the Animal Care and Use Committee at the University of Colorado Denver.

**Blood and urine chemistry.** Blood glucose levels were measured using a Glucometer Elite XL (Bayer, Tarrytown, NY). Plasma lipid levels was measured with kits from Wako Chemical (Richmond, VA). Urine albumin and creatinine concentrations were determined using kits from Exocell (Philadelphia, PA).

**Quantitative real-time PCR and Western blotting.** Quantitative PCR and Western blotting were performed as previously described (4–7). Primer sequences are available from the authors on request or can be found elsewhere (4–7). The antibody against α-smooth muscle actin ([α-SMA], Sigma, St. Louis, MO) was used at 1:1,000 dilution for Western blotting.

**Lipid extraction and measurement of lipid composition.** Lipids from the kidneys were extracted by the method of Bligh and Dyer, as we have previously described (4–7). Triglyceride and cholesterol composition were measured by gas chromatography (Agilent Technologies, Wilmington, DE).

**NF-κB transcriptional activity assay.** Nuclear protein extracts were prepared from kidney tissue and used for the measurement of NFκB transcriptional activity with a kit from Marligen Biosciences (Rockville, MD) according to the manufacturer's instructions.

**Oxidized protein analysis.** The amount of oxidized proteins in kidney homogenates was determined by using an OxyElisa Oxidized Protein Quantitation Kit (Millipore, Billerica, MA) according to the manufacturer's instructions.

**Histology staining, electron microscopy, and immunofluorescence microscopy.** Sections (4-μm thick) cut from 10% formalin-fixed, paraffin-embedded kidney samples were used for periodic acid-Schiff (PAS) staining and Masson's trichrome staining. Frozen sections were used for oil red O staining of neutral lipid deposits or for immunostaining for nephrin (a gift from Dr Larry Holzman, University of Michigan, Ann Arbor, MI), synaptopodin (Sigma), fibronectin (Sigma), CD68 (AbD Serotec, Raleigh, NC), and α-SMA (Sigma), and imaged with a laser scanning confocal microscope (LSM 510, Zeiss, Jena, Germany). The expression level was quantified as the sum of pixel values per glomerular area using ImageJ version 1.44 image analysis software. Electron microscopy (EM) was conducted in the Mouse Metabolic Phenotyping Center (University of Washington, Seattle, WA). Samples for EM were fixed in 1/2 x Karnovsky's fixative.

**Quantification of morphology.** All quantifications were performed in a masked manner. Using coronal sections of the kidney, 30 consecutive glomeruli per mouse, 6 mice per group were examined for evaluation of glomerular mesangial expansion. The index of the mesangial expansion was defined as the ratio of mesangial area/glomerular tuft area. The mesangial area was determined by assessment of the PAS-positive and nucleus-free area in the mesangium using ScanScope image analyzer (Aperio Technologies, Vista, CA).

**Statistical analysis.** Results are presented as the means ± SE for at least three independent experiments. Data were analyzed by ANOVA and Student-Newman-Keuls tests for multiple comparisons or by Student $t$ test for unpaired data between two groups. Statistical significance was accepted at the $P < 0.05$ level.

## RESULTS

**FXR deficiency accelerates diabetic nephropathy.** To investigate whether FXR plays a role in diabetic nephropathy and if FXR deficiency accelerates diabetic kidney injury, we induced insulin deficiency and hyperglycemia with STZ in FXR KO mice with the C57BL/6 genetic background. Progress of renal injury was compared with wild-type C57BL/6 mice injected with STZ, a mouse strain previously shown to be resistant to STZ-induced hyperglycemic kidney disease (15). To accelerate disease progression, we placed all mice on WD after they developed hyperglycemia. As shown in Table 1, STZ injections led to a marked increase in blood glucose level in both wild-type and FXR KO mice. Both wild-type mice and FXR KO mice injected with STZ had markedly low insulin levels. FXR deficiency without diabetes caused a mild increase in plasma triglyceride, total cholesterol, HDL cholesterol, and LDL cholesterol levels, compared with C57BL/6 wild-type mice. In contrast, a significant increase of plasma lipid level was observed in diabetic FXR KO mice on WD, associated with proatherogenic changes, including a decrease in HDL cholesterol, increase in LDL cholesterol, and the dominant LDL cholesterol level in total cholesterol.

Diabetic wild-type C57BL/6 mice did not show increased albuminuria, and there was only moderate albuminuria in nondiabetic FXR KO mice fed a WD. However, urinary albumin/creatinine ratio in FXR KO mice after 12 weeks of diabetes was markedly increased by 11-fold over diabetic wild-type C57BL/6 mice (Table 1). The development of albuminuria in diabetic FXR KO mice was associated with increased diabetes-induced renal hypertrophy compared with wild-type mice, but the difference did not reach statistical significance, as revealed by the kidney-to-body weight ratio (Table 1). However, the glomerular volume was significantly increased in diabetic FXR KO mice (Table 1).

Wild-type C57BL/6 mice or nondiabetic FXR KO mice showed nearly normal glomerular structure with only mild mesangial expansion (Fig. 1*A–C*). In contrast, the glomerular tufts in diabetic FXR KO mice exhibited foam cell accumulation with glomerular lobulation enlarging the entire glomerular area and more mesangial matrix expansion (Fig. 1*D–I*). Some capillaries were extended and occluded by foam cells or dilated and contained pale-

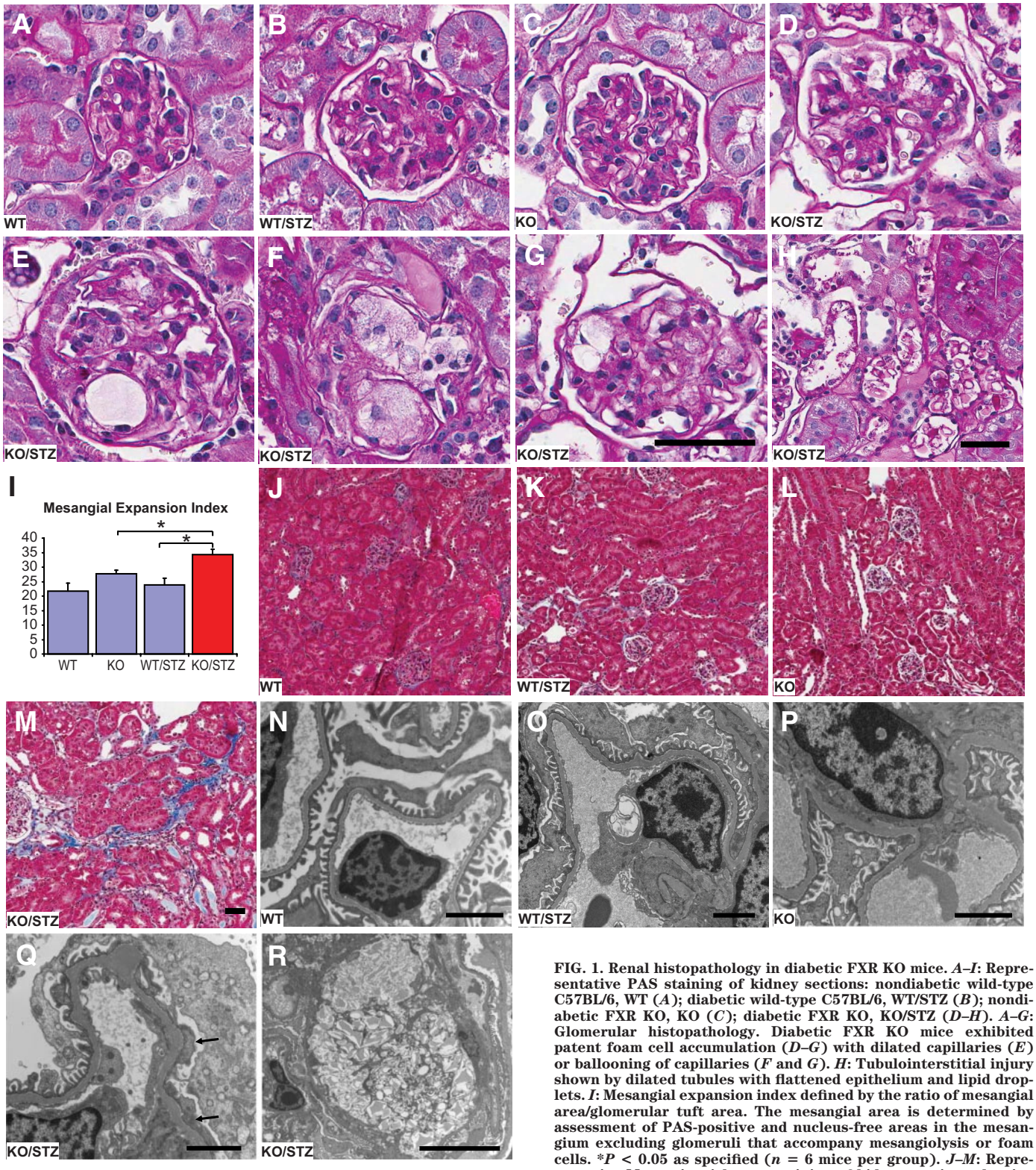


**FIG. 1. Renal histopathology in diabetic FXR KO mice. *A–I*: Representative PAS staining of kidney sections: nondiabetic wild-type C57BL/6, WT (*A*); diabetic wild-type C57BL/6, WT/STZ (*B*); nondiabetic FXR KO, KO (*C*); diabetic FXR KO, KO/STZ (*D–H*). *A–G*: Glomerular histopathology. Diabetic FXR KO mice exhibited patent foam cell accumulation (*D–G*) with dilated capillaries (*E*) or ballooning of capillaries (*F* and *G*). *H*: Tubulointerstitial injury shown by dilated tubules with flattened epithelium and lipid droplets. *I*: Mesangial expansion index defined by the ratio of mesangial area/glomerular tuft area. The mesangial area is determined by assessment of PAS-positive and nucleus-free areas in the mesangium excluding glomeruli that accompany mesangiolysis or foam cells. *$P < 0.05$ as specified ($n = 6$ mice per group). *J–M*: Representative Masson's trichrome staining of kidney sections showing the tubulointerstitial fibrosis in diabetic FXR KO mice. *N–R*: Electron micrographs of glomeruli showing reactive podocyte and endothelial cell (*Q*) and lytic mesangium (*R*) in diabetic FXR KO mice. Irregular thickening of GBM in *Q* indicates possible subepithelial deposit and increased vesicles in the podocyte cell body. *Arrows* in *Q* show effacement of podocyte foot processes. Lytic leision in *R* looks like lipid deposits or cholesterol "clefts." Scale bar: *A–G*, 50 μm (shown in *G*); *H*, 50 μm; *J–M*, 50 μm (shown in *M*); *N–Q*, 2 μm; *R*, 10 μm. (A high-quality digital representation of this figure is available in the online issue.)**

staining material (Fig. 1*E*). Some glomeruli displayed prominent mesangiolysis accompanied by ballooning of capillaries (Fig. 1*F* and *G*). In tubulointerstitial areas, wild-type mice or nondiabetic FXR KO mice showed no significant tubular damage, whereas diabetic FXR KO mice had remarkable tubulointerstitial changes. The tubules were dilated, lined by flattened epithelium, and contained proteinaceous casts with large amounts of lipid droplets

deposited in the tubular epithelial cells (Fig. 1*H*). Interstitial collagen deposition was studied in Masson's trichrome-stained renal sections as an index of interstitial fibrosis. Diabetic FXR KO mice showed more interstitial fibrosis than wild-type mice and nondiabetic FXR KO mice (Fig. 1*J–M*).

Electron microscopic examination from diabetic FXR KO mice disclosed increased podocyte and endothelial cell reactivity and local foot process effacement (Fig. 1*N–Q*). As shown in Fig. 1*R*, prominent mesangiolysis and lipid inclusions in the mesangium were observed, accompanied by dissociation of mesangial matrix and disruption of anchoring of glomerular basement membrane (GBM) to mesangium.

In agreement with lipid deposits and foam cell accumulation, immunofluorescence microscopy revealed an increase in CD68-positive macrophages in the glomeruli and tubulointerstitium in diabetic FXR KO mice compared with wild-type controls (Fig. 2*A*). This is associated with increased expression of master inflammatory mediator NFκB subunit p65 and elevated NFκB activation level (Fig. 2*B*).

An important mechanism causing albuminuria is podocyte dysfunction (16,17). Immunofluorescence microscopy showed that the distribution of podocyte markers, synaptopodin and nephrin, was changed from uniformly linear pattern in wild-type and nondiabetic FXR KO mice to discontinuous pattern with loss of staining in diabetic FXR KO mice (Fig. 2*C*). Nephrin is a key component of the slit diaphragm complex, and synaptopodin, a differentiated podocyte marker, is a regulator of actin dynamics for podocyte foot processes. Both are critically important for the sustained function of glomerular filtration barrier to proteinuria (16–18). Podocyte loss was also confirmed by staining with WT1, a nuclear podocyte marker, showing a significantly reduced podocyte density in diabetic FXR KO mice (Fig. 2*D*). Our results thus indicate podocyte loss, decreased podocyte density, and loss of podocyte differentiation markers in the kidneys of diabetic FXR KO mice.

**Increased renal expression of profibrotic growth factors and accumulation of matrix proteins in diabetic FXR KO mice.** Glomerulosclerosis and tubulointerstitial fibrosis are pathologic hallmarks of diabetic renal disease, characterized by accumulation in the kidney of extracellular matrix (ECM) proteins and myofibroblasts, the primary matrix-producing cells (19). TGF-β is a cytokine that plays a pivotal role in the profibrotic responses (20). In diabetic FXR KO mice, we found a significant increase of TGF-β mRNA expression in the kidney compared with corresponding wild-type or nondiabetic controls, in parallel with increased expression of microRNA-192 and decreased expression of microRNA-29a (Fig. 2*E*). MicroRNAs have been shown to be actively involved in TGF-β signaling. MicroRNA-192 is important for TGF-β–induced ECM production (21). MicroRNA-29 inhibits several mRNAs involved in ECM production and fibrosis (22). Our data suggest that TGF-β-induced increase in the expression of microRNA-192 coordinately downregulates microRNA-29a to control the induction of fibrosis gene expression related to the pathogenesis of diabetic nephropathy. We also examined the expression of ECM protein fibronectin by immunofluorescence, and found increased expression of fibronectin in glomeruli of diabetic FXR KO mice (Fig. 2*F*). FXR deficiency also increased the renal expression level of two myofibroblast markers, fibroblast-specific protein-1 (FSP-1) and α-SMA (Fig. 2*G*).

**Increased lipid accumulation in the kidneys of diabetic FXR KO mice.** We found that FXR deficiency caused increased kidney neutral lipid accumulation in both glomeruli and tubulointerstitium, as determined by oil red O staining, and biochemical lipid analysis revealed increased kidney triglyceride and cholesterol content (Fig. 3*A*). To explore the mechanism by which FXR regulates renal lipid accumulation, we investigated pathways regulating renal lipid metabolism. In glomeruli isolated from diabetic FXR KO mice, we found significantly increased expression of SREBP-1c and its target genes fatty acid synthase (FAS), acetyl-CoA carboxylase (ACC), and stearoyl-CoA desaturase-1 (SCD-1), which mediate fatty acid and triglyceride synthesis. In addition, we observed increased expression of LDL receptor and lectin-like oxidized LDL receptor-1 (LOX-1), which mediate cholesterol and oxidized LDL uptake (Fig. 3*B*).

**FXR activation protects against diabetic nephropathy.** To further confirm the role of FXR in diabetic nephropathy, we used the selective FXR agonist INT-747 to test whether the FXR activation can ameliorate diabetic nephropathy in a STZ-induced type 1 diabetes model. Because C57BL/6 mice are resistant to diabetic renal injury, STZ-injected nephropathy-susceptible DBA/2J mice were used (15). As shown in Table 2, STZ injections led to a marked increase in blood glucose level in DBA/2J mice. Diabetic DBA/2J mice developed increased triglyceride and cholesterol levels, with a marked increase in LDL cholesterol levels. Treatment with the selective FXR agonist INT-747 did not decrease the blood glucose level in diabetic DBA/2J mice, but it significantly decreased plasma total cholesterol and LDL cholesterol levels. No changes were observed in the HDL cholesterol and triglyceride levels (Table 2).

**Treatment with INT-747 decreases albuminuria and renal histopathology alterations in diabetic DBA/2J mice.** Diabetic DBA/2J mice on WD developed severe albuminuria, which was significantly decreased and nearly normalized by INT-747 treatment (Table 2). In diabetic DBA/2J mice, morphometric analysis revealed a moderate but significant increase of mesangial matrix expansion in glomeruli which was blunted by INT-747 treatment (Fig. 4*A–D*). Patchy fibrosis was demonstrated in the tubular interstitium of diabetic DBA/2J kidneys, but was nearly absent in the kidneys of mice treated with INT-747 (Fig. 4*E* and *F*).

In diabetic DBA/2J mice, immunofluorescence staining showed in the kidney reduced expression of synaptopodin, which was prevented by INT-747 treatment (Fig. 4*G*). Podocyte loss revealed by WT1 staining (Fig. 4*H*) in diabetic DBA/2J mice was also rescued by INT-747 treatment. Conversely, INT-747 treatment decreased renal Notch1 mRNA level which was enhanced in diabetic DBA/2J kidneys (Fig. 4*I*). As Notch activation in podocytes is involved in the development of proteinuria and podocyte dysfunction (23), these data suggest that INT-747 prevents the development of proteinuria by preventing podocyte dysfunction in DBA/2J mice.

**Treatment with INT-747 decreases profibrotic growth factors, accumulation of extracellular matrix, macrophage accumulation, and NADPH oxidase expression in diabetic DBA/2J mice.** In diabetic DBA/2J mice, INT-747 treatment blocked the increase of TGF-β expression in diabetic kidneys, suggesting that

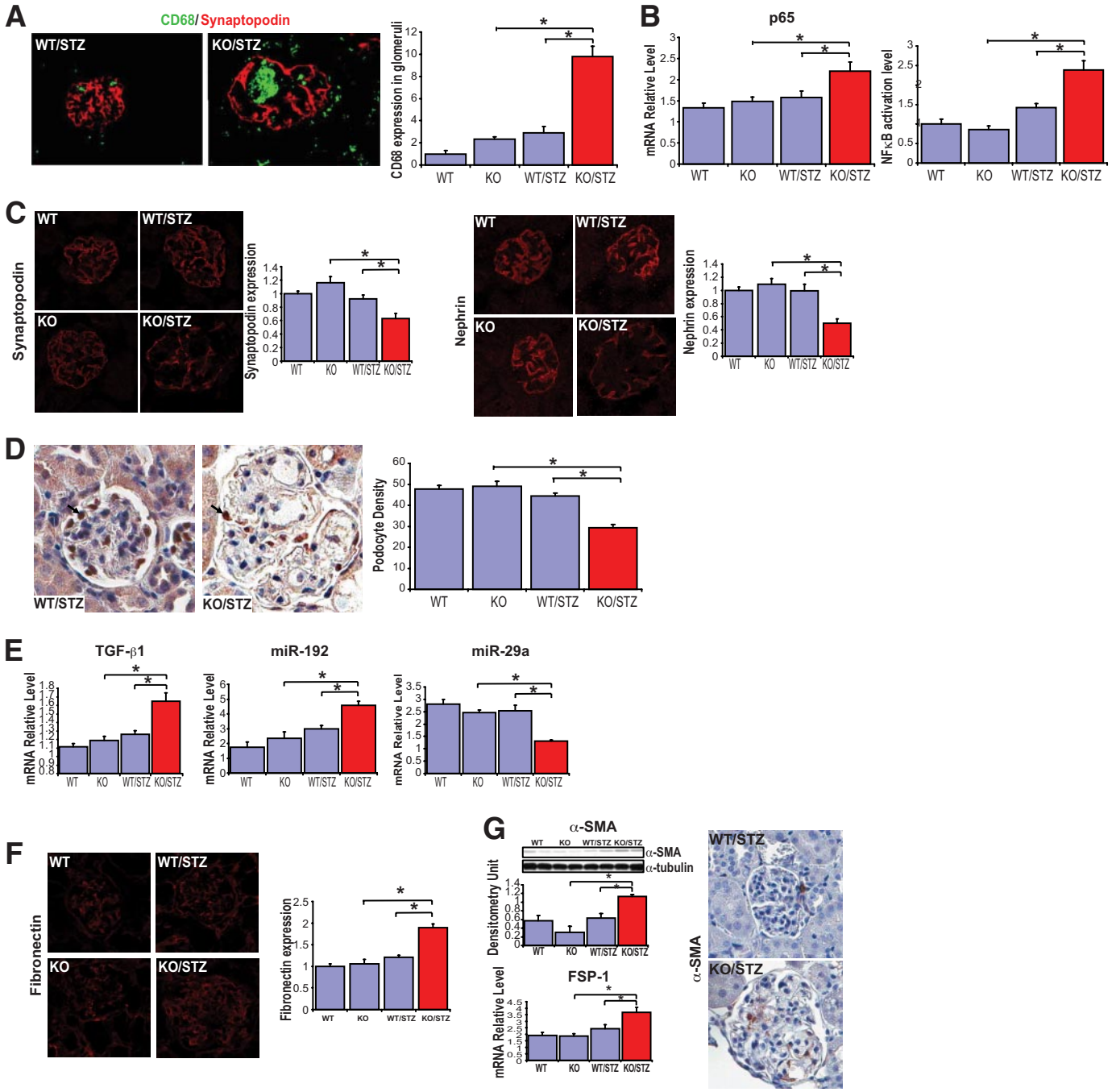


**FIG. 2. Macrophage infiltration and renal expression of podocyte markers, profibrotic growth factors, and extracellular matrix protein in diabetic FXR KO mice. *A*: Immunofluorescence staining of kidney sections for synaptopodin (red) and CD68 (green). The CD68 expression level in glomeruli was normalized to that in the wild-type group. *B*: Renal NF-κB p65 subunit mRNA expression by quantitative real-time PCR and NF-κB activation determined by DNA-binding assay. *C*: Immunofluorescence staining of kidney sections for synaptopodin and nephrin. The expression level of synaptopodin and nephrin was normalized to that in the wild-type group. *D*: Immunohistologic detection of WT1 in glomeruli. WT1 staining is indicated by intense immunoperoxidase activity in podocyte nuclei (*arrows*). Podocyte density is presented as the numbers of podocytes per glomerular area. *E*: Renal mRNA expression levels of TGF-β1, microRNA-192, and microRNA-29a determined by quantitative real-time PCR. F: Immunofluorescence staining of kidney sections for fibronectin. The expression level of fibronectin was normalized to that in the wild-type group. *G*: FSP-1 mRNA expression in kidney was determined by quantitative real-time PCR, and the protein level of α-SMA in the kidney demonstrated by Western blot and immunohistologic staining. *$P < 0.05$ as specified ($n = 6$ mice per group). (A high-quality digital representation of this figure is available in the online issue.)**

FXR activation may counteract kidney fibrosis induced by TGF-β (Fig. 5*A*). In addition, INT-747 treatment markedly inhibited fibronectin expression in glomeruli (Fig. 5*B*) and significantly reduced renal α-SMA and FSP-1 expression, which were both increased in diabetic DBA/2J mice (Fig. 5*C*). FXR activation markedly decreased the expression of macrophage marker CD68 in the glomeruli of diabetic kidneys (Fig. 5*D*), which was consistent with its inhibition in p65 expression and NFκB activity (Fig. 5*E*). INT-747 also modulated oxidative stress, as shown by decreased NADPH oxidase Nox-2 and p22-phox expression and total protein carbonylation in diabetic kidneys from INT-747-treated mice (Fig. 5*F*).

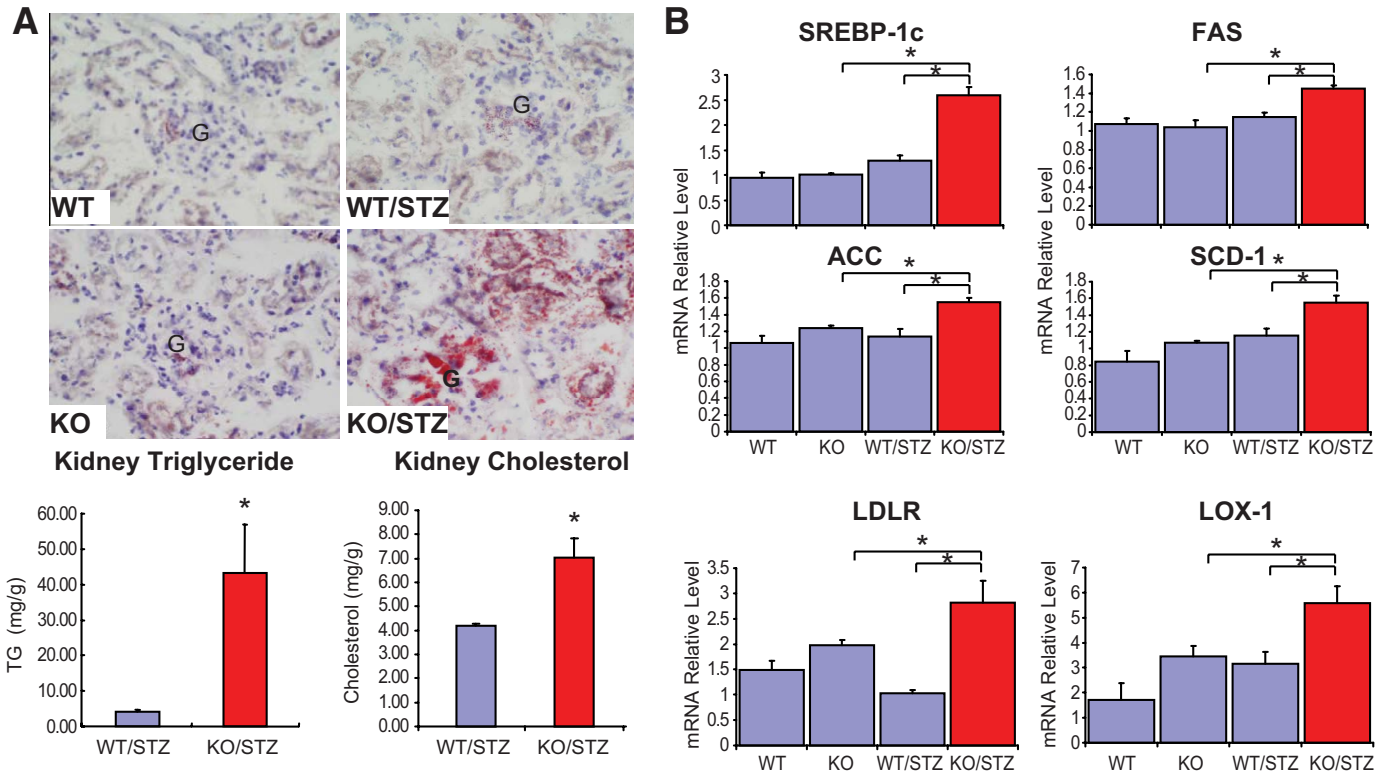


**FIG. 3. Diabetic FXR KO kidney showed increased lipid accumulation. *A*: Oil red O staining of kidney sections and kidney lipid content showing lipid accumulation in diabetic FXR KO kidneys. G, glomerulus. *B*: Analysis of renal mRNA expression by quantitative real-time PCR for SREBP-1c, FAS, ACC, SCD-1, LDLR, and LOX-1 in isolated glomeruli. *$P < 0.05$ vs. diabetic wild-type C57BL/6J mice on WD or as specified ($n = 6$ mice per group). (A high-quality digital representation of this figure is available in the online issue.)**

**Treatment with INT-747 decreases lipid accumulation in diabetic DBA/2J mice.** Diabetic DBA/2J mice had increased kidney neutral lipid accumulation in both glomeruli and tubulointerstitium and enhanced kidney triglyceride and cholesterol content. Treatment with INT-747 significantly attenuated kidney lipid accumulation (Fig. 6*A*). Correspondingly, glomerular lipid synthesis genes were downregulated, including: *1*) SREBP-1c and its target gene SCD-1, carbohydrate responsive element binding protein (ChREBP) and its target gene liver pyruvate kinase (LPK), which mediate fatty acid and triglyceride synthesis, and *2*) SREBP-2 which mediates cholesterol synthesis (Fig. 6*B*).

TABLE 2
Metabolic data in INT-747–treated diabetic mice

| | WD | STZ/WD | INT-747/ STZ/WD |
|---|---|---|---|
| Body weight (g) | 39.2 ± 1.40 | 17.6 ± 0.35[a] | 17.8 ± 1.27 |
| Kidney weight (g) | 0.46 ± 0.02 | 0.47 ± 0.02 | 0.48 ± 0.02 |
| Kidney/body weight ratio (%) | 1.16 ± 0.04 | 2.70 ± 0.11[a] | 2.72 ± 0.0 |
| Plasma glucose (mg/dl) | 179 ± 6 | 651 ± 26[a] | 637 ± 47 |
| Plasma TG (mg/dl) | 195 ± 46 | 955 ± 163[a] | 906 ± 142 |
| Plasma TC (mg/dl) | 297 ± 17 | 1,452 ± 137[a] | 782 ± 112[b] |
| Plasma HDL-C (mg/dl) | 93.6 ± 6.4 | 115 ± 26 | 98.7 ± 8.7 |
| Plasma LDL-C (mg/dl) | 24.0 ± 3.9 | 727 ± 96[a] | 364 ± 87[b] |
| Plasma insulin (ng/ml) | 8.73 ± 2.53 | 0.26 ± 0.04[a] | 0.20 ± 0.01 |
| Urine ACR (mg/g) | 88.0 ± 10.7 | 603 ± 113[a] | 106 ± 23[b] |

Data are means ± SE ($n = 6$ mice in each group): [a]$P < 0.05$ vs. WT + WD, [b]$P < 0.05$ vs. WT + STZ/WD. ACR, albumin/creatinine ratio; HDL-C, HDL cholesterol; LDL-C, LDL cholesterol; TC, total cholesterol; TG, triglyceride.

## DISCUSSION

The purpose of this study was to examine the role of the nuclear bile acid receptor FXR in diabetic nephropathy. The present data demonstrate accelerated renal injury in a model of experimental diabetic nephropathy in FXR KO mice on the nephropathy-resistant C57BL/6 background. In a type 1 diabetes model using the nephropathy-susceptible DBA/2J strain, renal injury was attenuated by FXR activation with the selective FXR agonist INT-747, suggesting that FXR plays a pivotal role in diabetic renal injury in these models.

Clinical observations have suggested that hyperlipidemia contributes to the progression of diabetic renal disease (24,25). To accentuate diabetic injury in the kidney, we have combined type 1 diabetes and hyperlipidemia by feeding WD to mice rendered diabetic with STZ. FXR deficiency triggers hypertriglyceridemia and hypercholesterolemia in diabetic C57BL/6 mice on WD, but not in nondiabetic mice. In addition, in diabetic mice FXR deficiency switches the lipid profile to pro-atherogenic by decreasing HDL cholesterol and increasing LDL cholesterol. The same degree of hyperlipidemia and lipid profile change is also observed in diabetic DBA/2J mice fed with WD. Interestingly, treatment with INT-747 decreases plasma cholesterol, but not triglyceride levels, in diabetic DBA/2J mice.

Our observations in the STZ-induced type 1 diabetes model are not consistent with FXR activation decreasing both plasma triglyceride and cholesterol levels (11,12,26),

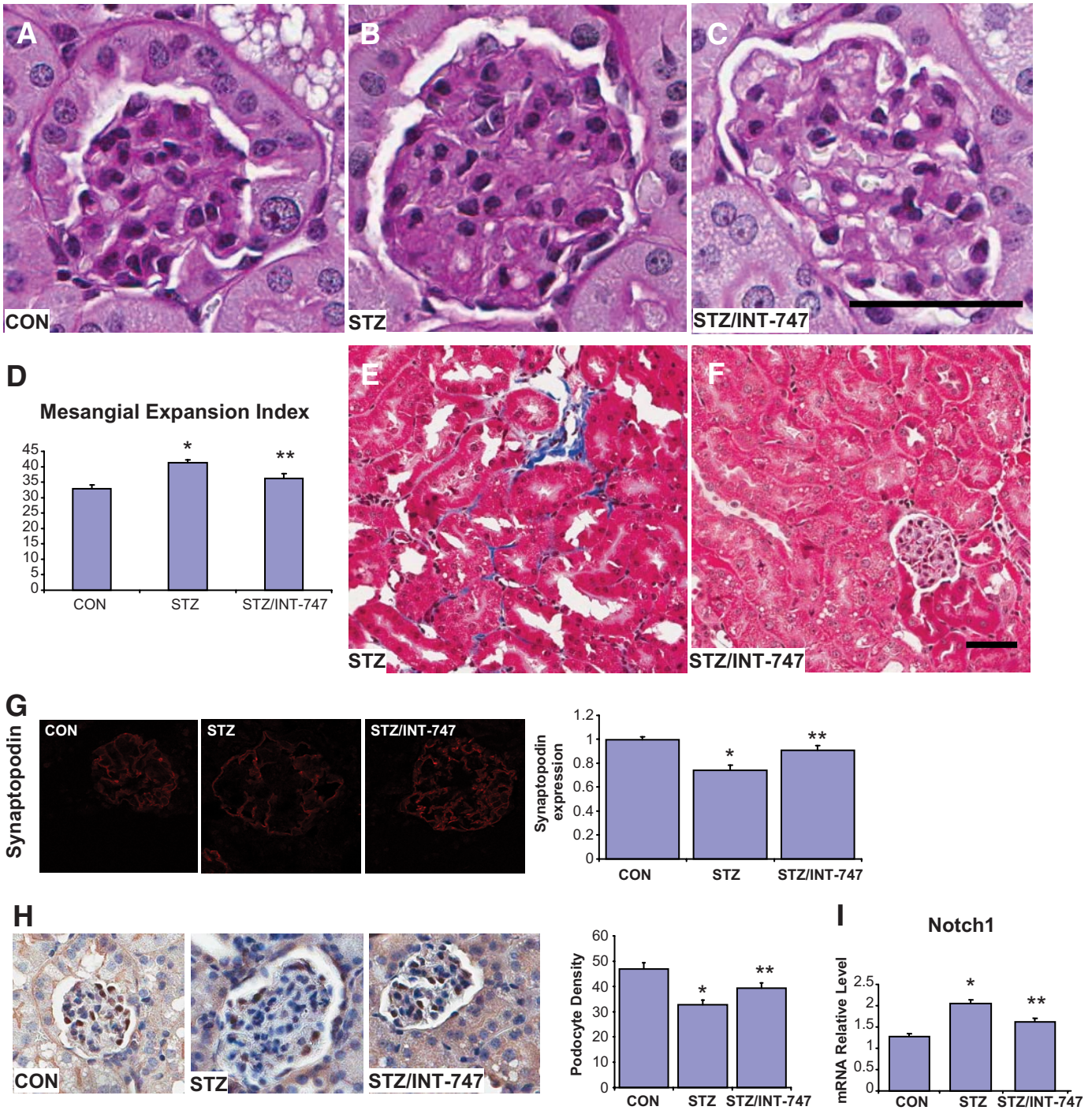


**FIG. 4. INT-747 treatment improves renal pathology in diabetic DBA/2J mice. *A–C*: Representative PAS staining of kidney sections: nondiabetic DBA/2J, CON (*A*); diabetic DBA/2J without treatment, STZ (*B*); diabetic DBA/2J treated with INT-747, STZ/INT-747 (*C*). *D*: Mesangial expansion index defined by the ratio of mesangial area/glomerular tuft area. The mesangial area is determined by assessment of PAS-positive and nucleus-free areas in the mesangium. *E* and *F*: Representative Masson's trichrome staining of diabetic FXR KO kidney sections showing tubulointerstitial fibrosis: diabetic DBA/2J without treatment (*E*); diabetic DBA/2J treated with INT-747 (*F*). *G*: Immunofluorescence staining of kidney sections for synaptopodin. The expression level of synaptopodin was normalized to that in the control group. *H*: Immunohistologic detection of WT1 in glomeruli. Podocyte density is presented as the numbers of podocytes per glomerular area. *I*: Notch1 renal mRNA expression level determined by quantitative real-time PCR. Scale bar: *A–C*, 50 μm (shown in *C*); *E* and *F*, 50 μm (shown in *F*). **P* < 0.05 vs. CON; ***P* < 0.05 vs. STZ (*n* = 6 mice per group). (A high-quality digital representation of this figure is available in the online issue.)**

and with the observation that FXR KO mice have increased plasma LDL and HDL levels (13,27). This may reflect lack of insulin-mediated regulation of genes controlling lipid homeostasis in STZ-induced diabetes (28). However, we cannot exclude the possibility that INT-747 mixed in the diet admix is less bioavailable compared with the gavage administration (12), blunting some of its effects.

The renal injury in diabetic FXR KO mice was associated with severe albuminuria as well as a variety of structural changes in both glomeruli and tubulointerstitium not seen in the nondiabetic counterpart or in diabetic

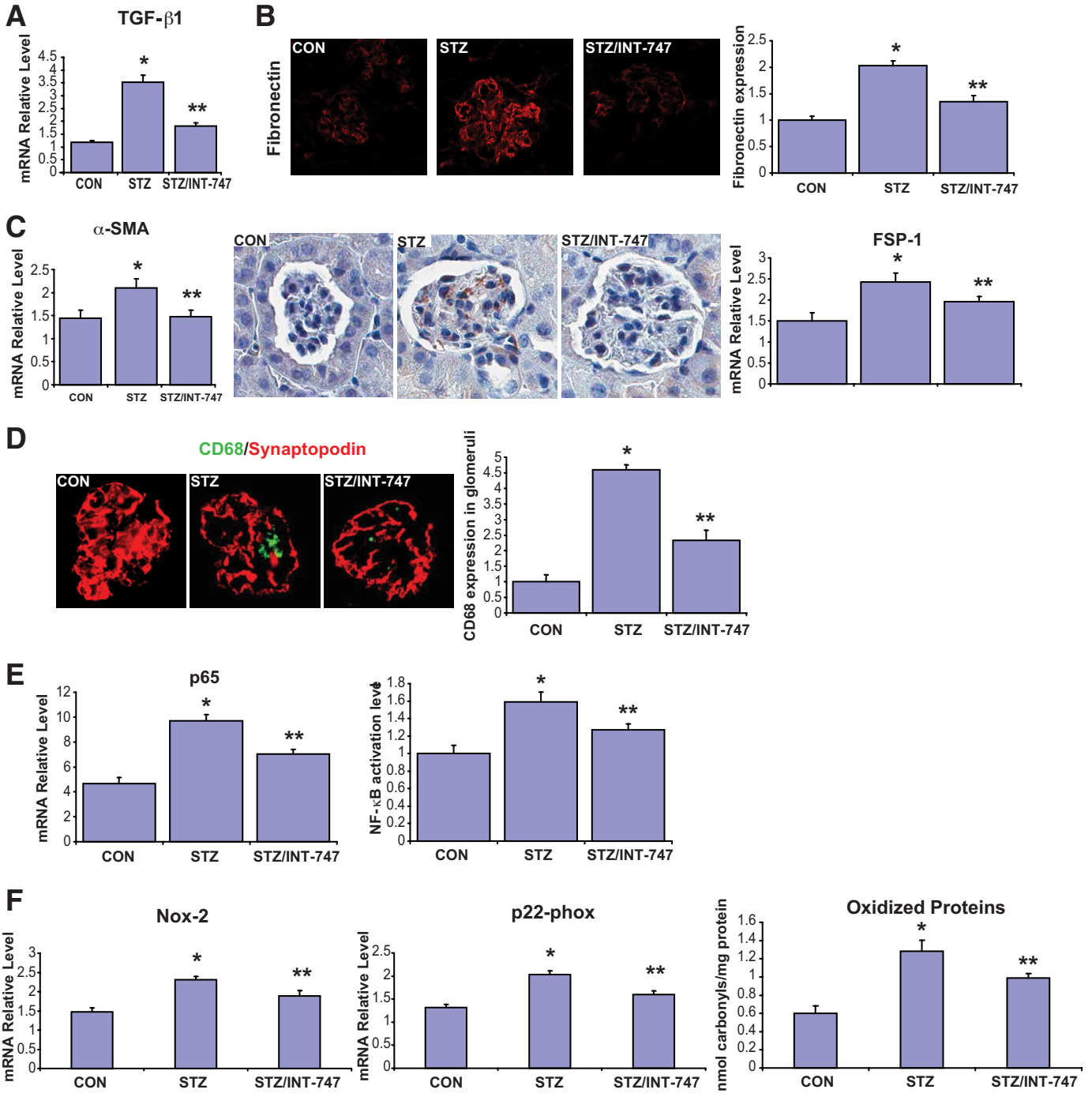


**FIG. 5. INT-747 treatment showed antifibrotic, anti-inflammatory, and antioxidative effects on diabetic DBA/2J mice. *A*: Renal TGF-β1 mRNA expression determined by quantitative real-time PCR. *B*: Immunofluorescence staining of kidney sections for fibronectin. The expression level of fibronectin was normalized to that in the control group. *C*: Expression of α-SMA in kidney determined by quantitative real-time PCR and immunohistologic staining. FSP-1 mRNA expression in kidney was determined by quantitative real-time PCR. *D*: Immunofluorescence staining of kidney sections for synaptopodin (red) and CD68 (green). *E*: Renal NF-κB p65 subunit mRNA expression by quantitative real-time PCR and NF-κB activation determined by DNA binding assay. *F*: Nox-2 and p22-phox mRNA expression in kidney determined by quantitative real-time PCR. Oxidative carbonylation of proteins in kidney homogenate was measured by ELISA. *$P < 0.05$ vs. CON; **$P < 0.05$ vs. STZ ($n = 6$ mice per group). (A high-quality digital representation of this figure is available in the online issue.)**

wild-type C57BL/6 mice. In this model we observed a large amount of lipid droplets and foam cell formation in the kidney, indicating an altered lipid homeostasis. There is growing evidence for the role of dysregulated lipid metabolism in the pathogenesis of renal disease (3–9,29). Previous studies in our laboratory have provided evidence that renal de novo lipid synthesis contributes to renal lipid accumulation in the pathogenesis of nephropathy (4–9,12). Although circulating lipids can amplify renal injury in diabetes, in a separate study with regular low-fat chow diet, diabetic FXR KO mice still exhibited increased proteinuria, mesangial expansion, and fibrosis, as shown by increased collagen III deposition compared with wild-type control mice (supplemental online Fig. S2). These results suggest that absence of FXR, even in the absence of a Western diet, can cause renal pathologic changes. The

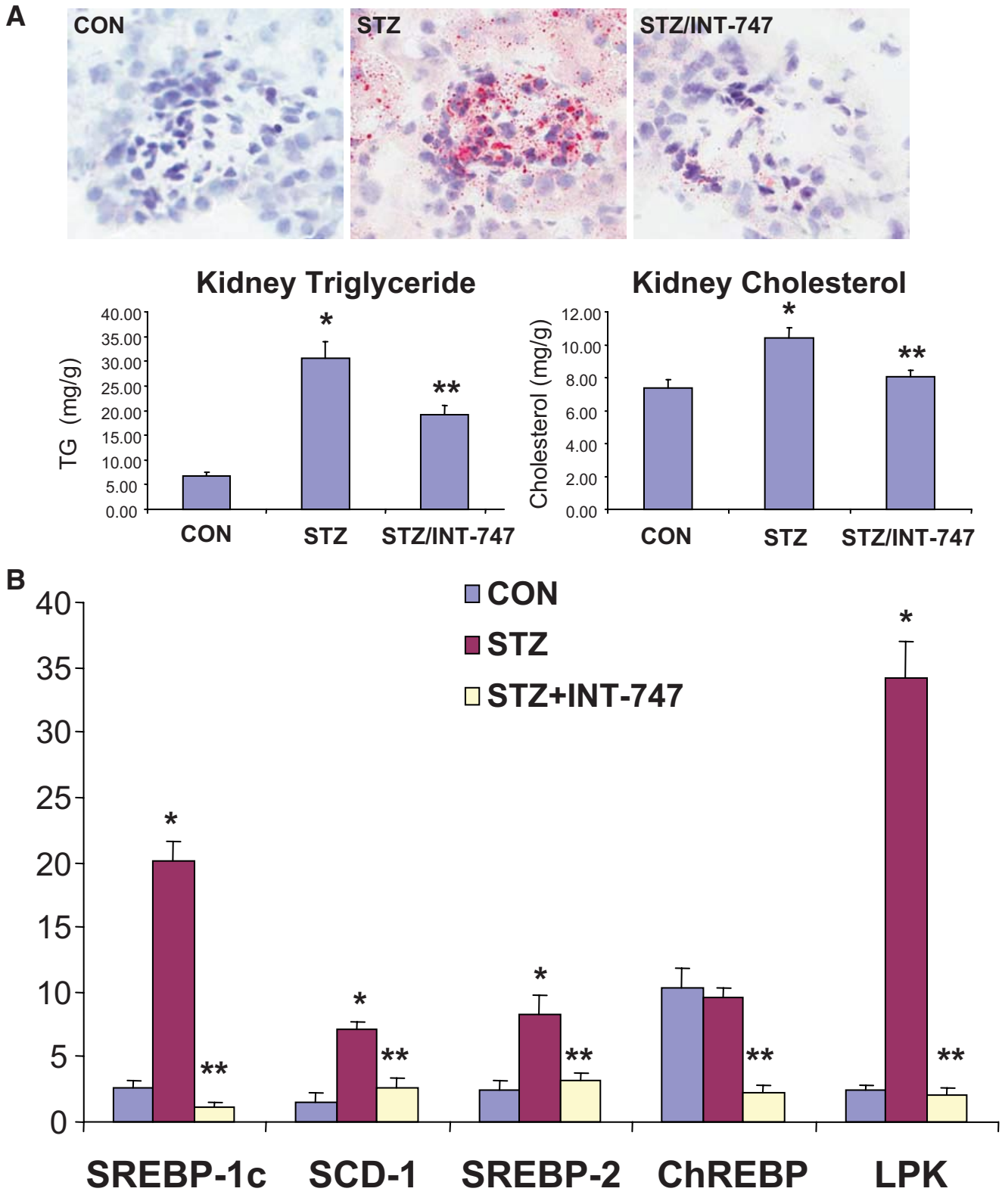


**FIG. 6. INT-747 treatment modulates lipid accumulation. *A*: Oil red O staining of kidney sections and kidney lipid content showing lipid accumulation in diabetic DBA/2J kidneys blunted by INT-747 treatment. *B*: Analysis of renal mRNA expression by quantitative real-time PCR for SREBP-1c, SCD-1, SREBP-2, ChREBP and LPK in isolated glomeruli. *$P < 0.05$ vs. CON; **$P < 0.05$ vs. STZ ($n = 6$ mice per group). (A high-quality digital representation of this figure is available in the online issue.)**

deleterious effects of FXR deficiency may result from disruption of FXR-regulated renal lipid metabolism or by other FXR-mediated actions, as the kidney expresses high FXR levels (7,30). We have shown before that FXR activation mediates negative regulation of SREBP-1-mediated renal lipid metabolism (7,12). Consistent with this observation, in the current study we found that FXR activation in DBA/2J mice with STZ-induced diabetes significantly

decreases glomerular expression of lipid synthesis genes, oil red O staining, as well as kidney lipid content. In addition, FXR deficient mice express more lipogenesis genes in glomeruli, indicating FXR-mediated regulation of renal lipid metabolism in diabetic FXR KO C57BL/6 mice as well as in diabetic DBA/2J mice.

Lipid metabolites can induce cellular dysfunction, a process known as lipotoxicity, to release profibrotic and proinflammatory cytokines and chemokines, increase the generation of reactive oxygen species, and promote the expression of extracellular matrix, contributing to oxidative stress, inflammation, and fibrosis in diabetic nephropathy (31–33). All these features were inhibited by INT-747 treatment in diabetic DBA/2J mice. Lipid products include oxidized and glycated LDLs, advanced glycation end products (AGEs), free fatty acids, free cholesterol, excess triacylglycerols, diacylglycerols, and ceramides. Kidney cells can acquire these lipids from atherogenic lipoproteins in circulation and intracellular lipid synthesis. All major cell types in kidney, including endothelial cells, monocyte–macrophages. and mesangial cells, have been shown to cause oxidative modification of LDL (34). Our study demonstrates upregulation of LDL receptor and LOX-1 expression in the glomeruli of diabetic FXR KO C57BL/6 mice, which can facilitate the LDL and oxidized LDL uptake, consistent with a previous report showing FXR-mediated regulation of LOX-1 in another diabetic mouse strain, KKAy (35). In obese rats with uncontrolled diabetes and dyslipidemia, renal LOX-1 upregulation promotes lipid peroxidation stress, inflammation, and fibrosis (36). Excess neutral lipid accumulation in mesangial cells and macrophages forms the lipid-laden foam cells that we have observed in kidneys from diabetic FXR KO mice. Foam cell formation is generally thought of as a protective mechanism whereby the potentially harmful lipids are sequestered in lipid droplets. However, recent evidence shows that genetic ablation of lipid droplets surface protein adipocyte differentiation-related protein (ADFP/adipophilin) expression restricts foam cell formation and protects mice against atherosclerosis development, suggesting that foam cell formation per se is a crucial pathogenic event (37). How foam cell accumulation affects the renal function is not fully understood. Based on our present findings, we speculate that severe foam cell accumulation in the mesangium leads to loss of mesangial support for normal capillary architecture, with consequent pathologic manifestations such as impaired glomerular filtration.

Development and progression of diabetic nephropathy are characterized by inflammatory infiltrates (38). The macrophage is a central mediator of renal vascular inflammation, and its accumulation is a feature of diabetic nephropathy (39–41). Macrophages mediate diabetic injury through a variety of mechanisms, including production of reactive oxygen species, cytokines, and proteases, which result in tissue damage leading to sclerosis and fibrosis (39–41). Components of the diabetic milieu, including high glucose, AGEs, and oxidized LDL, promote macrophage accumulation via induction of chemokines and adhesion molecules, and macrophage activation within diabetic kidneys (39–41). Our study shows that FXR deficiency increases macrophage infiltration in both glomeruli and tubulointerstitium, whereas treatment with the FXR agonist INT-747 reverses this course, both associated with regulation of NFκB activity. NFκB transcriptional activity controls the activation of a number of inflammatory genes. Consistent with our findings, the anti-inflammatory properties of INT-747 have been appreciated in other cell types (42,43). In vascular smooth muscle cells (42), the counterpart of glomerular mesangial cells, and in hepatocytes (43), INT-747 has been shown to inhibit the inflammatory response by antagonizing the NFκB signaling pathway. All together, this may represent a mechanism for FXR activation to inhibit inflammatory properties in macrophages and diabetic kidneys.

Our results show that proteinuria in diabetic mice is remarkably augmented by FXR deficiency, and significantly inhibited by FXR activation with INT-747. Damaging any component of the glomerular filtration barrier, fenestrated endothelium, intervening GBM, or slit diaphragms created by epithelial podocyte foot processes, results in proteinuria (16). Furthermore, mesangial cell injury can lead to foot process fusion and proteinuria (44). Tubules also play an important role in proteinuria by tubular reabsorption of filtered protein (16). FXR deficiency in diabetic mice showed the lytic mesangium with foamy cells, activated glomerular endothelium, and podocyte foot process effacement, indicating the involvement of multiple cell types in the pathogenesis of proteinuria in this model, as predicted by FXR expression in most kidney cell types. Indeed, the crosstalk of cytokines generated by mesangial cells, endothelial cells, and podocytes makes alterations in one cell type reverberate on others (44). Recently, FXR was found to directly enhance transcriptional activation of the endothelial nitric oxide synthase (*eNOS*) gene promoter, leading to increased nitric oxide production in vascular endothelial cells (45). This mechanism still remains to be ascertained in glomerular endothelial cells, but may represent a very important FXR-mediated effect, as eNOS deficiency results in endothelial dysfunction which favors development of diabetic nephropathy (46,47).

The diabetic FXR KO model does not recapitulate all typical features of human diabetic nephropathy, such as nodular mesangial lesions, although early lobulation was found in some glomeruli. This may relate to diabetes duration, resistant C57BL/6 background, or monogenic changes in gene expression intrinsic to this model, which makes it unable to reproduce full-fledged human diabetic nephropathy (48). However, the increased bile acid concentration in FXR KO mice (13) may lead to activation of the membrane bile acid receptor TGR5, a G-protein coupled receptor (49,50), which may exert compensatory actions in FXR deficiency (51). Establishing FXR deficiency in susceptible strains and exploring the role of TGR5 in diabetic nephropathy represent our future directions to clarify these issues and generate more predictive mouse models for human diabetic nephropathy.

In summary, our findings indicate a critical role for FXR in the development of diabetic nephropathy and show that FXR activation by the selective and potent FXR agonist INT-747 prevents nephropathy in type 1 diabetes by inhibiting diabetes-induced alterations in renal lipid metabolism, fibrosis, inflammation, and oxidative stress. This knowledge has translational potential into effective therapies for type 1 diabetic patients with diabetic renal complications.

**ACKNOWLEDGMENTS**

This work was supported by grants from the National Institutes of Health (NIH) (U01 DK-076134 and R01AG-

026529), Juvenile Diabetes Research Foundation, and the Veterans Affairs Merit Review. Y.C. was supported by a minority graduate student supplement from NIH and H.S. was supported by the LAB COATS Program at the University of Colorado Denver.

No potential conflicts of interest relevant to this article were reported.

X.X.W., T.J., Y.S., Y.C., S.M.-A., H.S., P.S., and L.L. researched data. X.X.W. wrote the manuscript. F.J.G. contributed to the discussion. L.A., J.B.K., J.W.V., M.P., and M.L. reviewed/edited the manuscript.

The authors would like to thank Kelly Hudkins, NIH Mouse Metabolic Phenotyping Center, University of Washington in Seattle, for assistance with histology staining and electron microscopy.

## REFERENCES

1. United States Renal Data System. Atlas of end-stage renal disease in the United States. In *USRDS 2009 Annual Data Report*. Bethesda, MD, 2009. Available from http://www.usrds.org/adr.htm. Accessed 24 August 2010
2. Brownlee M. The pathobiology of diabetic complications: a unifying mechanism. Diabetes 2005;54:1615–1625
3. Qian Y, Feldman E, Pennathur S, Kretzler M, Brosius FC 3rd. From fibrosis to sclerosis: mechanisms of glomerulosclerosis in diabetic nephropathy. Diabetes 2008;57:1439–1445
4. Sun L, Halaihel N, Zhang W, Rogers T, Levi M. Role of sterol regulatory element-binding protein 1 in regulation of renal lipid metabolism and glomerulosclerosis in diabetes mellitus. J Biol Chem 2002;277:18919–18927
5. Wang Z, Jiang T, Li J, Proctor G, McManaman JL, Lucia S, Chua S, Levi M. Regulation of renal lipid metabolism, lipid accumulation, and glomerulosclerosis in FVB db/db mice with type 2 diabetes. Diabetes 2005;54:2328–2335
6. Proctor G, Jiang T, Iwahashi M, Wang Z, Li J, Levi M. Regulation of renal fatty acid and cholesterol metabolism, inflammation, and fibrosis in Akita and OVE26 mice with type 1 diabetes. Diabetes 2006;55:2502–2509
7. Jiang T, Wang XX, Scherzer P, Wilson P, Tallman J, Takahashi H, Li J, Iwahashi M, Sutherland E, Arend L, Levi M. Farnesoid X receptor modulates renal lipid metabolism, fibrosis, and diabetic nephropathy. Diabetes 2007;56:2485–2493
8. Ishigaki N, Yamamoto T, Shimizu Y, Kobayashi K, Yatoh S, Sone H, Takahashi A, Suzuki H, Yamagata K, Yamada N, Shimano H. Involvement of glomerular SREBP-1c in diabetic nephropathy. Biochem Biophys Res Commun 2007;364:502–508
9. Jiang T, Wang Z, Proctor G, Moskowitz S, Liebman SE, Rogers T, Lucia MS, Li J, Levi M. Diet-induced obesity in C57BL/6J mice causes increased renal lipid accumulation and glomerulosclerosis via a sterol regulatory element-binding protein-1c-dependent pathway. J Biol Chem 2005;280:32317–32325
10. Watanabe M, Houten SM, Wang L, Moschetta A, Mangelsdorf DJ, Heyman RA, Moore DD, Auwerx J. Bile acids lower triglyceride levels via a pathway involving FXR, SHP, and SREBP-1c. J Clin Invest 2004;113:1408–1418
11. Zhang Y, Castellani LW, Sinal CJ, Gonzalez FJ, Edwards PA. Peroxisome proliferator-activated receptor-gamma coactivator 1α (PGC-1α) regulates triglyceride metabolism by activation of the nuclear receptor FXR. Genes Dev 2004;18:157–169
12. Wang XX, Jiang T, Shen Y, Adorini L, Pruzanski M, Gonzalez FJ, Scherzer P, Lewis L, Miyazaki-Anzai S, Levi M. The farnesoid X receptor modulates renal lipid metabolism and diet-induced renal inflammation, fibrosis, and proteinuria. Am J Physiol Renal Physiol 2009;297:F1587–F1596
13. Sinal CJ, Tohkin M, Miyata M, Ward JM, Lambert G, Gonzalez FJ. Targeted disruption of the nuclear receptor FXR/BAR impairs bile acid and lipid homeostasis. Cell 2000;102:731–744
14. Pellicciari R, Fiorucci S, Camaioni E, Clerici C, Costantino G, Maloney PR, Morelli A, Parks DJ, Willson TM. 6α-ethyl-chenodeoxycholic acid (6-ECDCA), a potent and selective FXR agonist endowed with anticholestatic activity. J Med Chem 2002;45:3569–3572
15. Qi Z, Fujita H, Jin J, Davis LS, Wang Y, Fogo AB, Breyer MD. Characterization of susceptibility of inbred mouse strains to diabetic nephropathy. Diabetes 2005;54:2628–2637
16. Jefferson JA, Shankland SJ, Pichler RH. Proteinuria in diabetic kidney disease: a mechanistic viewpoint. Kidney Int 2008;74:22–36
17. Ly J, Alexander M, Quaggin SE. A podocentric view of nephrology. Curr Opin Nephrol Hypertens 2004;13:299–305
18. Mundel P, Heid HW, Mundel TM, Kruger M, Reiser J, Kriz W. Synaptopodin: an actin-associated protein in telencephalic dendrites and renal podocytes. J Cell Biol 1997;139:193–204
19. Strutz F, Zeisberg M. Renal fibroblasts and myofibroblasts in chronic kidney disease. J Am Soc Nephrol 2006;17:2992–2998
20. Bottinger EP. TGF-β in renal injury and disease. Semin Nephrol 2007;27:309–320
21. Kato M, Zhang J, Wang M, Lanting L, Yuan H, Rossi JJ, Natarajan R. MicroRNA-192 in diabetic kidney glomeruli and its function in TGF-β-induced collagen expression via inhibition of E-box repressors. Proc Natl Acad Sci U S A 2007;104:3432–3437
22. van Rooij E, Sutherland LB, Thatcher JE, DiMaio JM, Naseem RH, Marshall WS, Hill JA, Olson EN. Dysregulation of microRNAs after myocardial infarction reveals a role of miR-29 in cardiac fibrosis. Proc Natl Acad Sci U S A 2008;105:13027–13032
23. Niranjan T, Bielesz B, Gruenwald A, Ponda MP, Kopp JB, Thomas DB, Susztak K. The Notch pathway in podocytes plays a role in the development of glomerular disease. Nat Med 2008;14:290–298
24. Hirano T. Lipoprotein abnormalities in diabetic nephropathy. Kidney Int 1999;71(Suppl.):S22–S24
25. Krolewski AS, Warram JH, Christlieb AR. Hypercholesterolemia–a determinant of renal function loss and deaths in IDDM patients with nephropathy. Kidney Int 1994;45 (Suppl.):S125–S131
26. Zhang Y, Lee FY, Barrera G, Lee H, Vales C, Gonzalez FJ, Willson TM, Edwards PA. Activation of the nuclear receptor FXR improves hyperglycemia and hyperlipidemia in diabetic mice. Proc Natl Acad Sci U S A 2006;103:1006–1011
27. Lambert G, Amar MJ, Guo G, Brewer HB, Jr, Gonzalez FJ, Sinal CJ. The farnesoid X-receptor is an essential regulator of cholesterol homeostasis. J Biol Chem 2003;278:2563–2570
28. Raghow R, Yellaturu C, Deng X, Park EA, Elam MB. SREBPs: the crossroads of physiological and pathological lipid homeostasis. Trends Endocrinol Metab 2008;19:65–73
29. Kume S, Uzu T, Araki S, Sugimoto T, Isshiki K, Chin-Kanasaki M, Sakaguchi M, Kubota N, Terauchi Y, Kadowaki T, Haneda M, Kashiwagi A, Koya D. Role of altered renal lipid metabolism in the development of renal injury induced by a high-fat diet. J Am Soc Nephrol 2007;18:2715–2723
30. Bookout AL, Jeong Y, Downes M, Yu RT, Evans RM, Mangelsdorf DJ. Anatomical profiling of nuclear receptor expression reveals a hierarchical transcriptional network. Cell 2006;126:789–799
31. Abrass CK. Cellular lipid metabolism and the role of lipids in progressive renal disease. Am J Nephrol 2004;24:46–53
32. Weinberg JM. Lipotoxicity. Kidney Int 2006;70:1560–1566
33. Prieur X, Roszer T, Ricote M: Lipotoxicity in macrophages: evidence from diseases associated with the metabolic syndrome. Biochim Biophys Acta 2010;1801:327–337
34. Ruan XZ, Varghese Z, Moorhead JF. An update on the lipid nephrotoxicity hypothesis. Nat Rev Nephrol 2009;5:713–721
35. Harnish D, Hahn A, Hartman H, Huard C, Martinez R, Mahaney P, Evans M, Zhang S. The farnesoid X receptor (FXR) antagonizes oxidized LDL receptor, LOX-1, activation (Abstract). Circulation 2007;116:II_161
36. Kelly KJ, Wu P, Patterson CE, Temm C, Dominguez JH. LOX-1 and inflammation: a new mechanism for renal injury in obesity and diabetes. Am J Physiol Renal Physiol 2008;294:F1136–F1145
37. Paul A, Chang BH, Li L, Yechoor VK, Chan L. Deficiency of adipose differentiation-related protein impairs foam cell formation and protects against atherosclerosis. Circ Res 2008;102:1492–1501
38. Galkina E, Ley K. Leukocyte recruitment and vascular injury in diabetic nephropathy. J Am Soc Nephrol 2006;17:368–377
39. Chow F, Ozols E, Nikolic-Paterson DJ, Atkins RC, Tesch GH. Macrophages in mouse type 2 diabetic nephropathy: correlation with diabetic state and progressive renal injury. Kidney Int 2004;65:116–128
40. Sassy-Prigent C, Heudes D, Mandet C, Belair MF, Michel O, Perdereau B, Bariety J, Bruneval P. Early glomerular macrophage recruitment in streptozotocin-induced diabetic rats. Diabetes 2000;49:466–475
41. Chow FY, Nikolic-Paterson DJ, Atkins RC, Tesch GH. Macrophages in streptozotocin-induced diabetic nephropathy: potential role in renal fibrosis. Nephrol Dial Transplant 2004;19:2987–2996
42. Li YT, Swales KE, Thomas GJ, Warner TD, Bishop-Bailey D. Farnesoid x receptor ligands inhibit vascular smooth muscle cell inflammation and migration. Arterioscler Thromb Vasc Biol 2007;27:2606–2611
43. Wang YD, Chen WD, Wang M, Yu D, Forman BM, Huang W. Farnesoid X receptor antagonizes nuclear factor κB in hepatic inflammatory response. Hepatology 2008;48:1632–1643
44. Schlondorff D, Banas B. The mesangial cell revisited: no cell is an island. J Am Soc Nephrol 2009;20:1179–1187

45. Li J, Wilson A, Kuruba R, Zhang Q, Gao X, He F, Zhang LM, Pitt BR, Xie W, Li S. FXR-mediated regulation of eNOS expression in vascular endothelial cells. Cardiovasc Res 2008;77:169–177
46. Zhao HJ, Wang S, Cheng H, Zhang MZ, Takahashi T, Fogo AB, Breyer MD, Harris RC. Endothelial nitric oxide synthase deficiency produces accelerated nephropathy in diabetic mice. J Am Soc Nephrol 2006;17:2664–2669
47. Nakagawa T, Sato W, Glushakova O, Heinig M, Clarke T, Campbell-Thompson M, Yuzawa Y, Atkinson MA, Johnson RJ, Croker B. Diabetic endothelial nitric oxide synthase knockout mice develop advanced diabetic nephropathy. J Am Soc Nephrol 2007;18:539–550
48. Brosius FC 3rd, Alpers CE, Bottinger EP, Breyer MD, Coffman TM, Gurley SB, Harris RC, Kakoki M, Kretzler M, Leiter EH, Levi M, McIndoe RA, Sharma K, Smithies O, Susztak K, Takahashi N, Takahashi T. Mouse models of diabetic nephropathy. J Am Soc Nephrol 2009;20:2503–2512
49. Maruyama T, Miyamoto Y, Nakamura T, Tamai Y, Okada H, Sugiyama E, Nakamura T, Itadani H, Tanaka K. Identification of membrane-type receptor for bile acids (M-BAR). Biochem Biophys Res Commun 2002;298:714–719
50. Kawamata Y, Fujii R, Hosoya M, Harada M, Yoshida H, Miwa M, Fukusumi S, Habata Y, Itoh T, Shintani Y, Hinuma S, Fujisawa Y, Fujino M. A G protein-coupled receptor responsive to bile acids. J Biol Chem 2003;278:9435–9440
51. Thomas C, Pellicciari R, Pruzanski M, Auwerx J, Schoonjans K. Targeting bile-acid signalling for metabolic diseases. Nat Rev Drug Discov 2008;7:678–693